LETTERS
PUBLISHED ONLINE: 23 JANUARY 2011 | DOI: 10.1038/NGEO1069
nature geoscience

Catastrophic dispersion of coal fly ash into oceans during the latest Permian extinction

Stephen E. Grasby[1]*, Hamed Sanei[1] and Benoit Beauchamp[2]

During the latest Permian extinction about 250 Myr ago, more than 90% of marine species went extinct, and biogeochemical cycles were disrupted globally[1]. The cause of the disruption is unclear, but a link between the eruption of the Siberian Trap flood basalts and the extinction has been suggested on the basis of the rough coincidence of the two events[2,3]. The flood basalt volcanism released CO_2. In addition, related thermal metamorphism of Siberian coal measures and organic-rich shales led to the emission of methane, which would have affected global climate and carbon cycling, according to model simulations[2–6]. This scenario is supported by evidence for volcanic eruptions and gas release in the Siberian Tunguska Basin[6], but direct indicators of coal combustion have not been detected. Here we present analyses of terrestrial carbon in marine sediments that suggest a substantial amount of char was deposited in Permian aged rocks from the Canadian High Arctic immediately before the mass extinction. Based on the geochemistry and petrology of the char, we propose that the char was derived from the combustion of Siberian coal and organic-rich sediments by flood basalts, which was then dispersed globally. The char is remarkably similar to modern coal fly ash, which can create toxic aquatic conditions when released as slurries. We therefore speculate that the global distribution of ash could have created toxic marine conditions.

Our study focuses on the Buchanan Lake section, from the rapidly subsiding Sverdrup Basin, Canadian High Arctic (Fig. 1), which records uninterrupted and uncondensed Late Carboniferous to Cretaceous deep-water, bathyal to near abyssal, marine sedimentation across the latest Permian extinction (LPE) event on the NW margin of Pangea[7–10]. The section is dominated by fissile black siliceous shale of the Late Permian Black Stripe Formation that transitions to thinly laminated green Early Triassic Blind Fiord Formation shale[9]. The LPE boundary is marked by a significant negative shift in the $\delta^{13}C$ record of organic matter, consistent with other marine and terrestrial inorganic and organic records observed globally[8,11,12]. The boundary section is characterized by progressive development of basin-to-shelf anoxic to euxinic seawater that developed in response to chemocline upward excursion[8,9]. We present here petrographic and geochemical analyses (Supplementary Methods) of shale-hosted organic matter across the LPE event boundary at Buchanan Lake.

Microscopic examination of whole rock samples reveals two distinct groups of organic matter that are not discernable from hand sample or outcrop. Group 1 consists of thermally-altered liptinitic-origin matter (normal marine organics) and over-mature microscopic bitumen derived from them, with reflectance <3%. These reflectance values are consistent with regional thermal maturation studies that place Buchanan Lake in a Thermal Alteration Index (TAI) of 4, on the basis of spore and conodont colour alteration, as well as vitrinite reflectance[13]. Thermal maturation values of group 1 organics thus reflect the maximum regional burial-temperature of the host shale and are consistent with these organics having a primary marine origin. Group 2 organic matter consists of combustion-derived isotropic chars that commonly show high optical reflectance (>4%). These optical properties indicate intense, high-temperature carbonization and rapid combustion of organic material that cannot be associated with burial-related thermal maturation.

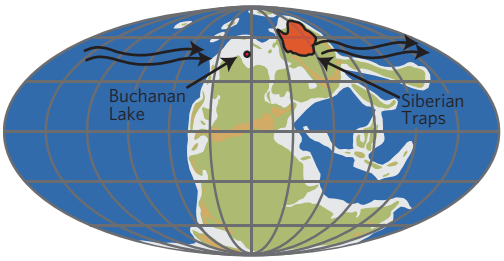

Figure 1 | Late Permian paleogeographic map showing location of the Buchanan Lake section and Siberian Traps volcanics. Lava flows combust coal beds through explosive eruption that inject ash into the stratosphere, where prevailing westerly winds transport it to the Sverdrup Basin (base map after R. Scotese).

Combusted coal and burnt wood have distinct optical features that allow them to be distinguished (Supplementary Organic Petrography). Several features of group 2 organics show a strong resemblance to modern fly ash collected from coal-fired power plants (Fig. 2), including: (1) carbon cenospheres with trapped inclusions of gas (Fig. 2a), (2) bulky inertinitic chars showing characteristic cracking related to rapid heating (Fig. 2b–d), and (3) highly vacuolated, spongy vitrinitic chars (Fig. 2e). Cenospheres are formed only by injection of molten coal into the atmosphere, causing rapid temperature quenching and hence 'freezing' in a spherical shape[14]. On the basis of these characteristic optical features, we interpret group 2 organics as originating from combusted coal.

Recycling of coal from contemporaneous or older Sverdrup Basin units, or from older strata of the underlying Franklinian Basin, cannot explain the abundant occurrence of the coaly particles, as coal is either very rare or non-existent[15]. Neither are there known Middle or Late Permian coal occurrences immediately west, south or north of the Sverdrup Basin that could explain the coal ash occurrence[16]. Given the position of the Sverdrup Basin, west of the vast Angara coal province of Siberia (Fig. 1), we considered Siberian Trap volcanism[2–6] as a feasible source for coal fly ash. At this latitude, with predominant westerlies, fly ash would have to travel >20,000 km eastward to reach the Sverdrup

[1]Geological Survey of Canada—Calgary, 3303 33rd Street N.W., Calgary Alberta, T2L 2A7, Canada, [2]Arctic Institute of North America, University of Calgary, 2500 University Dr. N.W., Calgary Alberta, T2N 1N4, Canada. *e-mail: sgrasby@nrcan.gc.ca.

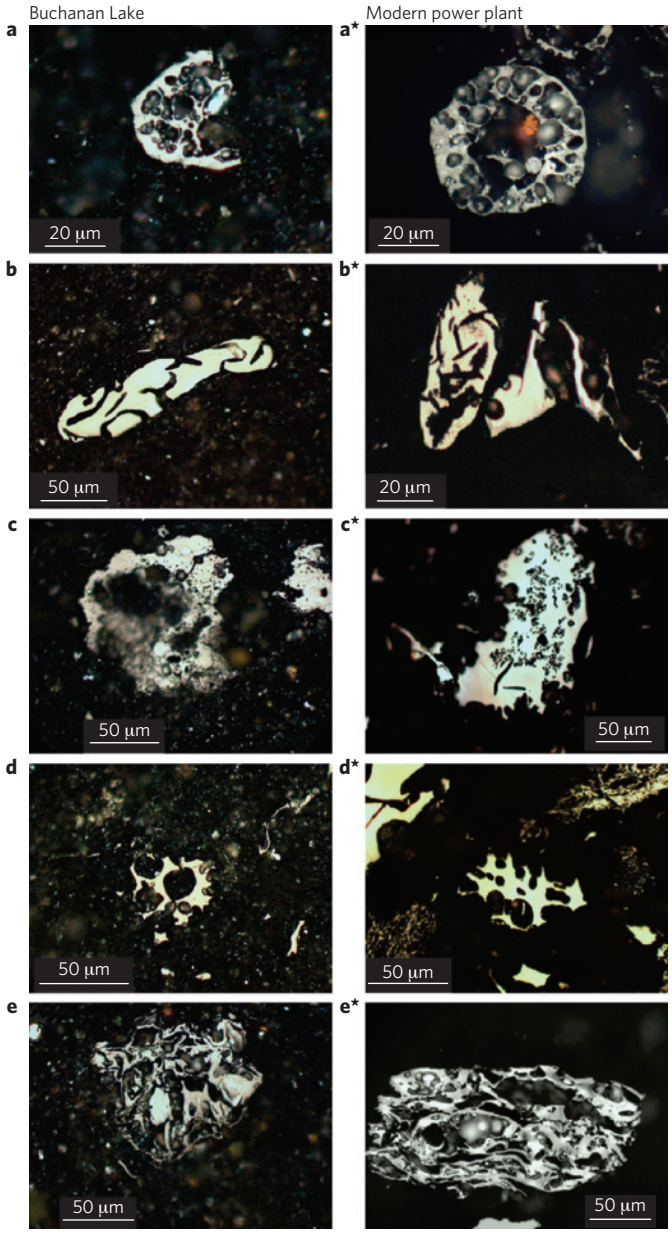

Figure 2 | Photomicrographs of combustion-derived isotropic chars. Chars from late Permian shales at Buchanan Lake (**a**–**e**) and their identical pairs in fly ash samples obtained from modern coal-fired power plants (**a***–**e***) are shown. Specific examples include (**a**–**a***): a carbon cenesophere with trapped inclusions of gas, showing the typical morphology of coal fly ash; (**b**–**b***, **c**–**c***, **d**–**d***): bulky inertinitic chars showing some precursor coal inertinite structure with the characteristics of cracking and deformation related to intense rapid heat; (**e**–**e***): highly vacuolated, spongy vitrinitic chars. Photographs are taken using reflected-light microscopy with immersion oil.

Basin. The majority of particles we observe are <50 µm, and cenospheres are <20 µm, within the fine to very fine volcanic ash size. Volcanic ash from this size range has been dispersed over thousands of kilometres in recent eruptions[17]. The Siberian Traps was a megascale eruption (more than 1,000 Gt of magma released), one of the largest in Earth history[3], and has associated high-velocity explosive release structures[6] as well as evidence for significant coal combustion[2–6]. Dispersion of ash is a function of the initial plume height (related to eruption magnitude), particle density, and wind speed. Flood basalt eruptions initiate with an explosive phase that

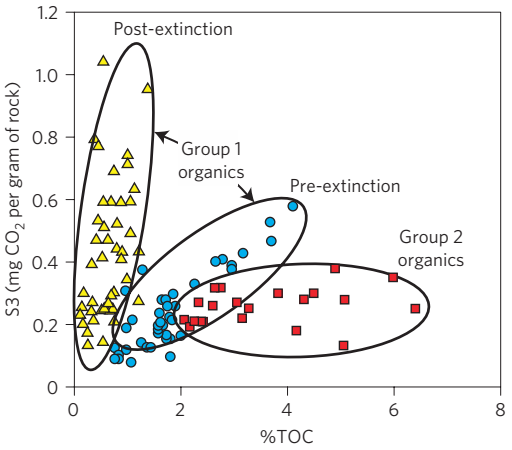

Figure 3 | Plot of S3 versus %TOC showing three distinct trends that relate to organic matter type. Group 2 organics (red squares) represent coal-derived combustion chars whereas group 1 represents background marine organics, showing a significant change in character across the LPE event from pre-extinction (blue circles) to postextinction (yellow triangles) samples.

can generate plumes over 20 km high, sufficient to inject ash into the stratosphere[18], and major eruptions with plumes >40 km are known. Cenosphere density is about half that of lithic fragments, meaning that coal fly ash entrained during eruption would be more widely dispersed. Transport towards the Sverdrup Basin would be favoured by strong mid-latitude westerly winds, making the Siberian Traps the most reasonable source of coal fly ash.

Our finding provides the first direct evidence for coal ash at the LPE event. Coal ash may not have been previously recognized elsewhere, as it is observed only through organic petrography. Modelling indicates that megascale eruptions may have formed interhemispheric ash clouds[19], allowing global coal ash distribution. The 'black organics particles' observed at Meishan[20] may support this. However the remarkable deep water record at Buchanan Lake, downwind of the Siberian Traps, may have uniquely favoured fly ash preservation.

To better define fly ash loading rates, speciation of organic carbon was determined by Rock-Eval Analyses. Figure 3 plots S3 (mg CO_2 per gram of rock) values, which represents the quantity of oxygen containing organic matter, against total organic carbon (%TOC). The slope of the regression line in the S3: TOC plot represents the oxygen index (OI) (S3/TOC × 100), which is proportional to the O:C ratio of the sedimentary organic matter. The result shows three groups of organic matter, as indicated by their distinct data regressions in the S3: TOC graph (Fig. 3). Two trends show typical variable development of S3 peaks as a function of TOC throughout the sedimentary succession. These trends are characteristic of kerogen-type marine organic matter that has undergone burial-induced thermal maturation, as represented by group 1 organics. There is a distinct shift in the S3: TOC data trends for samples above and below the LPE event boundary that is probably attributable to major changes in the kerogen composition (as indicated by OI) of autochthonous organic matter across the extinction horizon[21], related to global stresses on the marine ecosystem. The third trend shows samples with variable to high TOC values but with little S3 development. This reflects loading of highly refractory group 2 char.

Figure 4 shows temporal trends in %TOC at Buchanan Lake, distinguishing the three endmembers defined in Fig. 3, along with some key geochemical parameters. There is a general increase in autochthonous marine organic content going upwards towards the LPE boundary, associated with increased development of anoxia, as

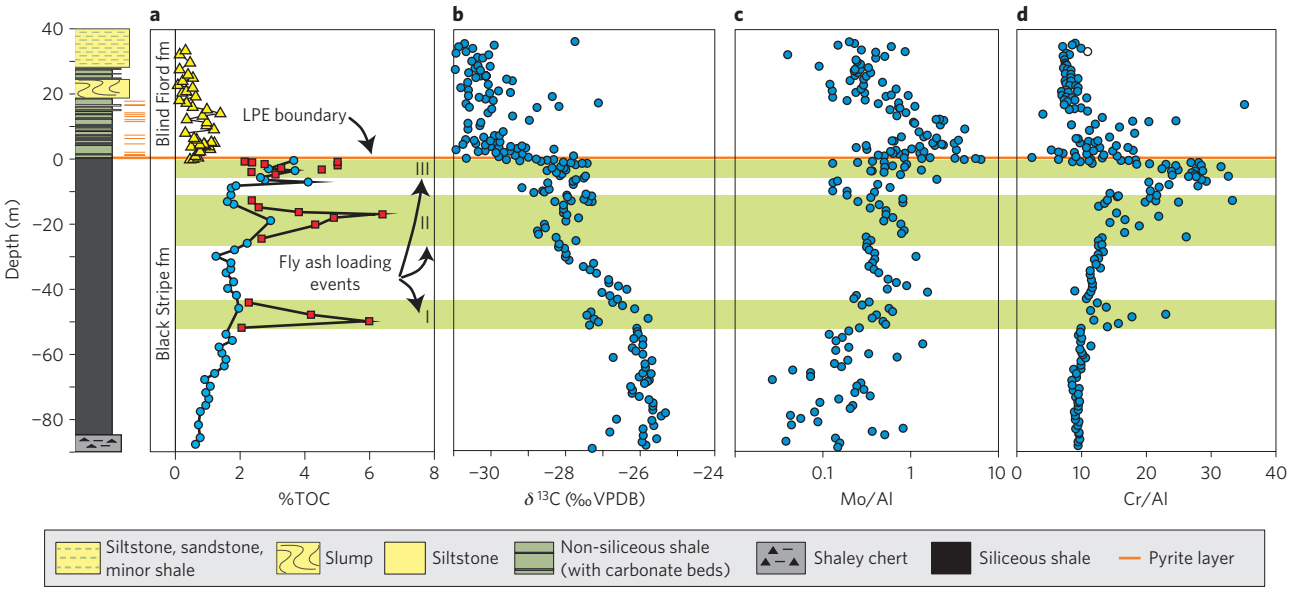

Figure 4 | Plot of vertical trends in key geochemical parameters across the LPE event at Buchanan Lake along with a lithostratigraphic column. Zones with high concentrations of combusted coal (horizontal green bars) are indicated as fly ash loading events. Vertical trends in **a** per cent total organic carbon (TOC%) are distinguished by symbols as defined in Fig. 3. Previously published[9] stable isotope and geochemical data (**b**–**d**) are also shown.

shown by increased Mo/Al ratios, followed by an abrupt drop across the boundary, consistent with the collapse of primary productivity associated with the extinction event. Most intriguing are 3 main loading events (I, II and III) of coal fly ash, as indicated by an abrupt increase in group 2 organics (red squares). On the basis of sedimentation rates we approximate the first loading event as 500–750 kyr before the LPE. Fly ash loading events dominate the TOC content at these times (confirmed by optical petrography), and as would be expected, cause a brief shift in the carbon isotope record (to ~−27‰) as the $\delta^{13}C_{org}$ value becomes temporally dominated by the fly ash component. Outside of fly ash loading events $\delta^{13}C_{org}$ records background trends in the marine biogeochemical carbon cycle as represented by group 1 autochthonous organic matter. $\delta^{13}C_{org}$ in the lowest part of the section is stable. After loading event I, there starts a progressive negative shift in $\delta^{13}C_{org}$, then a briefer negative shift after loading event II, and finally a large shift in $\delta^{13}C$ associated with the LPE event boundary after loading event III. This shows that globally observed shifts in $\delta^{13}C$ are a direct response to Siberian Trap volcanism. Although release of volcanic gas and ash to the atmosphere may be a cause of this link, we also consider the potential impact of coal fly ash loading on land and into ocean basins.

Mafic megascale eruptions are long-lived events that would allow significant build-up of global ash clouds[18]. More than 3 trillion tons of carbon released by Siberian Traps coal burning has been suggested[5,6]. The peak loading of pyrolytic carbon at Buchanan Lake (7%) indicates that fly ash slurries may have negatively impacted the chemistry of the Sverdrup Basin. With very low settling velocities, suspended coal ash particles form slurries that limit light penetration, whereas nutrients and toxic metals associated with fly ash are released into waters. Naturally occurring toxic and radioactive elements in coal are significantly concentrated into the fly ash component during combustion (for example ~98× concentration factor for As; refs 22,23). Even with modern emission control systems that capture up to 99% of ash content at coal-fired power plants, trace elements released from the remaining 1% are suggested to equal the natural flux from rock weathering[24]. Fly ash is known to stress aquatic ecosystems by generating anoxic conditions through limited photosynthesis and enhanced microbial activity, and metal toxicity[25]. Given this, coal ash dispersed by the explosive Siberian Trap eruption would be expected to have an associated release of toxic elements in impacted water bodies where fly ash slurries developed.

Chromium is enriched by a factor of ten to fifty times in modern coal fly ash[22]. The Cr/Al plot in Fig. 4 (corrected for changes in sediment flux by normalizing with Al) shows toxic metal release coinciding with each fly ash loading event. There are no changes in lithology associated with loading events to indicate an intrabasinal source (Fig. 4). Peak Cr levels occur during fly ash loading event III, just below the LPE boundary. At the same time, following each fly ash loading event, there is a shift to higher Mo/Al ratios, whereas $\delta^{13}C_{org}$ drops, suggesting increased development of anoxia as well as disruption of the biogeochemical carbon cycle in response to fly ash loading. Development of the highest Mo/Al values occurs at the LPE, immediately after fly ash loading event III. Here a significant change in character and size distribution of pyrite framboids has been interpreted as indicating the onset of euxinia at the LPE boundary[9]. Globally, biomarker evidence shows expansion of planktonic cyanobacteria communities associated with the LPE event, and this has been suggested to be at least partly related to enhanced nutrient inputs[21,26]. Models also show increases in nutrient flux are required for the onset of anoxia and euxinic conditions in Permian sea water[27]. Loading of nutrient rich fly ash (for example Fe) could provide a direct causal link between Siberian Trap volcanism and the development of anoxia.

Our study provides the first direct temporal link between thermal metamorphism of coal beds and the LPE event, supporting a causal relationship. Our results are consistent with other studies that suggest the onset of extinction[20,28], as well ocean anoxia[29,30], initiated before the LPE boundary. A key finding in our work is that negative $\delta^{13}C$ shifts occur after each fly ash loading event, including the large globally observed shift at the LPE boundary. This probably represents longer-term release of low $\delta^{13}C$ CO_2 from thermal metamorphism of coal and organic rich shales through smoldering groundfires, after the initial explosive eruption that generated the coal ash. It needs to be discerned further if this also reflects stress induced on the marine ecosystem by fly ash loading. Release of highly concentrated metals and nutrients in fly ash may have placed significant stress on the Sverdrup Basin and, potentially, the global ecosystem.

Received 2 September 2010; accepted 21 December 2010; published online 23 January 2011

References

1. Erwin, D. H. *Extinction. How life on Earth Nearly Ended 250 Million Years Ago* 296 (Princeton Univ. Press, 2006).
2. Reichow, M. K. *et al.* The timing and extent of the eruption of the Siberian Traps large igneous province: Implications for the end-Permian environmental crisis. *Earth Planet. Sci. Lett.* **277,** 9–20 (2009).
3. Saunders, A. D. & Reichow, M. K. The Siberian Traps and the end-Permian mass extinction: A critical review. *Chin. Sci. Bull.* **54,** 20–37 (2009).
4. Korte, C. *et al.* Massive volcanism at the Permian–Triassic boundary and its impact on the isotopic composition of the ocean and atmosphere. *J. Asian Earth Sci.* **37,** 293–311 (2010).
5. Retallack, G. J. & Jahren, A. H. Methane release from igneous intrusion of coal during Late Permian extinction events. *J. Geol.* **116,** 1–20 (2008).
6. Svensen, H. *et al.* Siberian gas venting and the end-Permian environmental crisis. *Earth Planet. Sci. Lett.* **277,** 490–500 (2009).
7. Beauchamp, B. *et al.* Late Permian sedimentation in the Sverdrup Basin, Canadian Arctic: The Lindström and Black Stripe formations. *Can. Soc. Petrol. Geol. Bull.* **57,** 167–191 (2009).
8. Grasby, S. E. & Beauchamp, B. Intrabasin variability of the carbon-isotope record across the Permian–Triassic transition, Sverdrup Basin, Arctic Canada. *Chem. Geol.* **253,** 141–150 (2008).
9. Grasby, S. E. & Beauchamp, B. Latest Permian to Early Triassic basin-to-shelf anoxia in the Sverdrup Basin, Arctic Canada. *Chem. Geol.* **264,** 232–246 (2009).
10. Embry, A. F. & Beauchamp, B. in *The Sedimentary Basins of Unites States and Canada* (ed. Miall, A. D.) 451–472 (Elsevier, 2008).
11. Baud, A., Magaritz, M. & Holser, W. T. Permian–Triassic of the Tethys; Carbon isotope studies. *Geol. Rundschau* **78,** 649–677 (1989).
12. Retallack, G. J. & Krull, E. S. in *Wetlands Through Time* Vol. 399 (eds Greb, S. F. & DiMichele, W. A.) 249–268 (Spec. Pap. Geol. Soc. Am., 2006).
13. Utting, J., Goodarzi, F., Dougherty, B. J. & Henderson, C. M. B. *Thermal maturity of Carboniferous and Permian rocks of the Sverdrup Basin, Canadian Arctic Archipelago*, Geol. Sur. Can., Paper no. 89–19 (1989).
14. Goodarzi, F. & Hower, J. C. Classification of carbon in Canadian fly ashes and their implications in the capture of mercury. *Fuel* **87,** 1949–1957 (2008).
15. Harrison, J. C. *Melville Island's salt-based fold belt, Arctic Canada* Geol. Sur. Can., Bull. **472,** (1995).
16. Rees, P. M. *et al.* Permian phytogeographic patterns and climate data/model comparisions. *J. Geol.* **110,** 1–31 (2002).
17. Cas, R. A. F. & Wright, J. V. *Volcanic Successions, Modern and Ancient* (Chapman, 1987).
18. Thordarson, T., Rampino, M., Keszthelyi, L. P. & Self, S. in *Preservation of Random Megascale Events on Mars and Earth: Influence on Geologic History* Vol. 453 (eds Keszthelyi, M. G. & L. P., Chapman) 37–53 (Special Paper Geol. Soc. Am., 2009).
19. Baines, P. G., Jones, M. T. & Sparks, R. S. J. The variation of large-magnitude volcanic ash cloud formation with source latitude. *J. Geophys. Res.* **113,** D21204 (2008).
20. Xie, S. *et al.* Changes in the global carbon cycle occured as two episodes during the Permina–Triassic crisis. *Geology* **35,** 1083–1086 (2007).
21. Grice, K. *et al.* Photic zone euxinia during the Permian–Triassic superanoxic event. *Science* **307,** 706–709 (2005).
22. Klein, D. H. *et al.* Pathways of thirty-seven trace elements through coal-fired power plant. *Environ. Sci. Technol.* **9,** 973–979 (1975).
23. Papastefanou, C. Escaping radioactivity from coal-fired power plants (CPPs) due to coal burning and the associated hazards: A review. *J. Environ. Radioact.* **101,** 191–200 (2010).
24. Bertine, K. K. & Goldberg, E. D. Fossil fuel combustion and the major sedimentary cycle. *Science* **173,** 233–235 (1971).
25. Rowe, C. L., Hopkins, W. A. & Congdon, J. D. Ecotoxicological implications of aquatic disposal of coal combustion residues in the United States: A review. *Environ. Monit. Assess.* **80,** 207–276 (2002).
26. Xie, S., Pancost, R. D., Yin, H., Wang, H. & Evershed, R. P. Two episodes of microbial change coupled with Permo/Triassic faunal mass extinction. *Nature* **434,** 494–497 (2005).
27. Hotinski, R. M., Bice, K. L., Kump, L. R., Najjar, R. G. & Arthur, M. A. Ocean stagnation and end-Permian anoxia. *Geology* **29,** 7–10 (2001).
28. Jin, Y. G. *et al.* Pattern of marine mass extinction near the Permian–Triassic boundary in south China. *Science* **289,** 432–436 (2000).
29. Twitchett, R. J., Looy, C. V., Morante, R., Visscher, H. & Wignall, P. B. Rapid and synchrous collapse of marine and terrestrial ecosystems during the end-Permian biotic crisis. *Geology* **29,** 351–354 (2001).
30. Wignall, P. & Newton, R. Contrasting deep-water records from the Upper Permian and Lower Triassic of South Tibet and British Columbia; evidence for a diachronous mass extinction. *Palaios* **18,** 153–167 (2003).

Acknowledgements

L. Stasiuk and J. Potter provided valuable scientific input. Helpful comments from Norm Sleep are appreciated. Geological Survey of Canada GCS Contribution 20100284.

Author contributions

S.E.G. collected field samples and conducted geochemical analyses, H.S. performed organic petrography, B.B. provided regional stratigraphic context.

Additional information

The authors declare no competing financial interests. Supplementary information accompanies this paper on www.nature.com/naturegeoscience. Reprints and permissions information is available online at http://npg.nature.com/reprintsandpermissions. Correspondence and requests for materials should be addressed to S.E.G.